

---

# Optimization and Power Management of Solar PV-based Integrated Energy System for Distributed Green Hydrogen Production

---

Sheikh Suhail Mohammad\* and Sheikh Javed Iqbal

*Department of Electrical Engineering, National Institute of Technology Srinagar, JK, India*

*E-mail: suhail\_46phd17@nitsri.net; jvd@nitsri.net*

*\*Corresponding Author*

Received 20 September 2021; Accepted 04 November 2021;  
Publication 22 April 2022

## **Abstract**

Photovoltaic-based integrated energy systems act as a possible modern technological solution for clean and affordable green hydrogen production. However, research attempts are required from the scientific community to develop power management, control, optimization algorithms, and new techniques for these integrated energy systems effective and economical operation. The integrated energy system considered in this work consists of a solar photovoltaic, battery, grid and proton exchange membrane (PEM) electrolyzer. PEM electrolyzer with a power rating of 100 kW is modelled as a controlled current sink to interfere with the DC bus directly. This work proposes a power management and control algorithm for the photovoltaic-based integrated energy system considering different parameters like availability of solar photovoltaic power, DC link voltage, battery state of charge (SOC), tariff and availability of grid power. Effective power-sharing among the different power sources increases system reliability and stability.

*Distributed Generation & Alternative Energy Journal, Vol. 37\_4, 865–898.*

doi: 10.13052/dgaej2156-3306.3741

© 2022 River Publishers

Optimization is performed for optimal sizing and costing to achieve economical operation such that these photovoltaic-based integrated energy systems become affordable and are encouraged for wide use. The photovoltaic system operates at the maximum power point through a neural network-based control strategy; in addition to this, stacking in neural network topologies is also discussed for improving system accuracy in tracking the reference voltage for MPPT operation. The DC link voltage is controlled by interfacing the battery with the DC link via a bidirectional buck-boost power converter. The contribution of the work is to highlight the role of renewable energy sources for continuous green hydrogen production. Green hydrogen will be a critical driving force for the future transportation system, fuel cell-based power generation, and industries utilizing hydrogen in direct or indirect forms—that will help transition towards a carbon-free society. Optimization and time-domain simulation results indicated the economic and technical feasibility of the proposed photovoltaic-based integrated energy system for green hydrogen production with the best optimal configuration producing hydrogen at the cost of \$ 4.806/kg and total net present cost of \$749904.

**Keywords:** Solar photovoltaic, battery, electrolyzer, grid, DC-DC converter, optimization, power management and control.

## 1 Introduction

In the present context, all the nations are framing their power and energy policies keeping in view the environmental challenges associated with fossil fuel-based power generation. It is clear that fossil fuel-based power generation produces a lot of emissions, the focus shifts towards renewable energy-based power and gas generation. The challenge remains how to achieve a smooth, reliable and affordable transition towards renewable power generation and hydrogen production in the presence of newly emerging energy sources, storage devices, and loads [1, 2].

Presently renewable energy based-power is being generated through microgrids (micropower systems). A microgrid consists of different power sources, energy storage devices, and different types of loads [3]. Based on the nature of the power generated by the power sources and the type of load, microgrids are broadly classified as AC, DC and AC-DC microgrids [4]. DC microgrids have advantages like high efficiency and reduced conversion stages than their AC counterparts. In addition to these advantages, DC power sources can feed power directly to new DC loads like electric vehicle

loads and electrolyzers. There are many renewable energy sources like solar power, wind power, fuel cell power etc.; among them, solar photovoltaic and wind are considered non-dispatchable power sources, and a fuel cell is a dispatchable power source [5]. In order to overcome the intermittency of non-dispatchable power sources, they are integrated with dispatchable power sources like fuel cells. Fuel cell finds their application in renewable microgrids and electric vehicles, electric trains, electric aeroplanes, etc., but hydrogen is vital for its operation. Not only for the applications mentioned, but hydrogen finds its use in industries also. Hence, there is a need to research and develop new ways of green hydrogen production.

There are many ways to generate hydrogen, as could be found in the literature. However, depending on the method of hydrogen generation, it is classified as a green, blue or brown fuel. Hydrogen is considered as a green fuel only when it is generated by PEM electrolyzer through some green energy power source [6,7]. It is put in the blue or brown category if generated by the reformers, where the source of heat and power is some fossil fuel. In [8], an electrical equivalent circuit was modelled and developed for the proton exchange membrane (PEM) electrolyzer and discussed the relationship between the hydrogen production rate and the input power and current. In [9], a 20 MW hydrogen production plant was installed in Canada; apart from this location currently, across the world, pilot testing is carried out for the large scale water electrolysis ranging from 10–100 MW hydrogen plants. At present, hydrogen infrastructure development has focused on locations where the grid has significant renewable energy penetration. Hence, provide support for grid stability and also leads to maximum utilization of renewable power [10]. As per the present statistical information about hydrogen production, only 5% of total hydrogen is produced through water electrolysis at the cost of 3–10 \$/kg. The other key indicators like efficiency, cost, power consumption, lifetime etc. regarding green hydrogen production can be found in [11]. Based on the current literature, it has been established that the attention is towards the large scale hydrogen production at the grid level. However, the need of the hour is to investigate the hydrogen production at a smaller scale so that the small scale consumers can participate in hydrogen production apart from power production at the distribution level. Hydrogen-based applications in power, transportation, health, and industrial sectors will be encouraged and widely used, therefore, leading a smooth transition towards a sustainable and green world.

Renewable energy-based microgrids for hydrogen production are associated with a lot of challenges. Some of the difficulties related to these

micropower systems are; to overcome the system uncertainty related to solar photovoltaic and wind power and to find the optimal size and cost of the system components. Many optimization models have been used for optimal sizing and costing of PV-based hybrid systems in the previous literature. In [12], implemented a mixed-integer linear programming optimization technique modelled in python for the optimization of the energy and power system. Authors in [13] used HOMER for the optimal design and analysis of charging station consisting of PV-wind-diesel generator, the charging station is analysed for both stand-alone mode of operation and grid-connected mode. Researchers in [14] performed the optimization of a grid-connected hybrid energy system for a residential house in Iran using HOMER considering both thermal and electric load growth rates. In yet another study [15] HOMER was used for the optimal design of PV-based system considering load growth and PV depreciation rates. A proper comparison was made to compare emission levels for stand-alone and grid connected energy systems. In [16], HOMER-based optimization was used for optimal sizing and costing for PV/Wind hybrid system. Authors in [17], studied the different climatic regions of Iran and carried out the feasibility analysis of PV/Wind/battery/grid-based different system configurations employing HOMER, so that utilisation of renewable energy resources is increased. The uncertainty associated with the solar photovoltaic system is overcome by integrating battery energy storage systems and developing different system architectures incorporating more than one power and energy storage device. Renewable energy-based microgrids are integrated with the power networks to increase the system reliability and the profit. Depending upon the scale of power production of microgrids, they are integrated with the grid at transmission or at the distribution level. However, integrating microgrids with the grid complicates the system control and operation. Power management and control algorithms are required to control these integrated complex systems. In [18], explained wind and the solar-based standalone hybrid system with different power management topologies; the extra power after serving the local load demand was utilized for hydrogen generation employing water electrolysis. In [19], developed energy management and control strategy for a hybrid system consisting of PV, wind and battery with battery state of charge as the primary control parameter. In [20], a power management strategy was developed for a hybrid system consisting of PV, wind, fuel cell and battery for electrification of remote loads. The main parameter for power management was battery SOC, and fuzzy logic-based control was used for extracting maximum power from wind turbines. For newly emerging power systems consisting of PV,

wind, fuel cell and energy storage devices, different power management and control strategies are designed; the details can be found in [21–26]. From the literature, the takeaway is that most papers have discussed and modelled electrolyzers in the power and control strategies as dump loads. However, modern time demands to model the electrolyzer as a critical load to maintain the continuous supply chain of hydrogen. Modelling the hydrogen production plants as critical loads need modification in power and control strategies for renewable energy-based microgrids.

In this work, the focus is to develop a small scale 100 kW water electrolysis-based hydrogen plant. This plant gets its power from the solar photovoltaic system during the daytime and from the local distribution network during night hours. Operating the hydrogen production plants during the night hours on-grid power reduces the cost of hydrogen production. In addition to cost reduction, it also provides ancillary services to the power networks with renewable energy power penetration. Optimization helps to find the optimal size and cost of the system components of the proposed integrated energy system. The proposed power management and control algorithm balance the system so that uninterrupted and economical hydrogen is produced, enhancing consumer participation in power and gas generation. The overall contribution of the paper is summarised as:

- Integrated energy system consisting of Solar PV, battery, grid and electrolyzer is proposed for distributed green hydrogen production.
- Technical and economic analysis is performed for the proposed system configuration to evaluate system feasibility, optimal sizing and costing.
- Power management algorithm is proposed for power balance and maximum utilisation of renewable power sources. It helps to overcome uncertainty associated with solar PV power and supply uninterrupted and stable rated power to PEM electrolyzer.
- To check the effectiveness of the proposed power management algorithm time-domain simulations are performed in MATLAB/Simscape environment.
- Optimization and time-domain simulations results indicate economic and technical feasibility of distributed green hydrogen production.

The rest of the paper is structured as follows. Section 2 defines the system configuration with a description of each system component, and Section 3 explains the optimization process for obtaining the best system configurations. Section 4 illustrates the power management and control algorithm for economic hydrogen production. The power electronic interface for each power source and energy storage is explained in Section 5. Time-domain

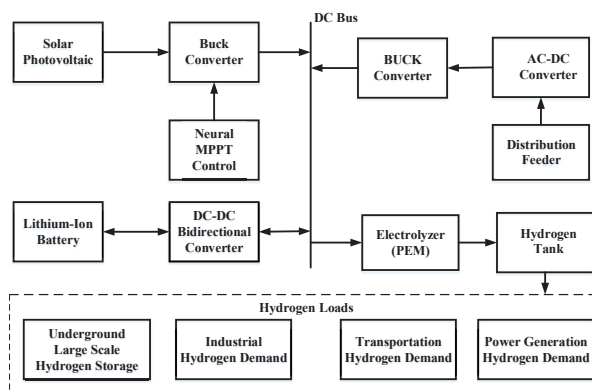


**Figure 1** Proposed system configuration for hydrogen production.

simulation results are presented in Section 6, followed by a conclusion in Section 7. Section 8 gives the future research direction.

## 2 System Configuration and Description for Integrated Energy System

To enhance the consumer participation in distributed generation-based combined power and gas production, system configuration as shown in Figure 1 is proposed. The system configuration consists of a solar photovoltaic system, battery energy storage, PEM electrolyzer, distribution feeder and associated power converters. PEM electrolyzer is designed and modelled as a non-linear DC-load. The proposed system configuration is carbon and sound free, making these systems suitable for installation in any residential or commercial area.

For the effective and successful working of the proposed system configuration: optimization, power management, and system control is vital. Optimization finds the optimal size and cost of the hybrid system configuration. Power management and control algorithms help control the power flow in the system and perform correct switching actions based on the knowledge of different control and decision variables. The optimal sizing and costing calculations are calculated using Benchmark software HOMER (Hybrid Optimization of Multiple Energy Resources) developed by the National Renewable Energy Laboratory (NREL) US. Apart from optimization, HOMER performs hourly time series simulations and sensitivity analysis of the micropower

system based on economic and technical grounds. Although HOMER has many advantages, its limitation is that it cannot perform the transient analysis. Therefore, events like switching of power sources and loads can not be performed in HOMER but through time-domain simulations performed in MATLAB/Simulink. The proposed custom-based power management and control algorithm implemented in the MATLAB/Simulink platform led to economic operation and increased system reliability & stability.

### 2.1 Solar Photovoltaic

Solar photovoltaic is one of the modern technologies that convert solar energy into electric energy. This energy conversion is an environmentally friendly process, where solar energy is converted to electric energy by solar panels made of crystalline silicon. An appropriate series-parallel combination of solar modules is needed to develop solar arrays of proper voltage and power rating. Different diode models model solar cells, but in this work, a solar cell is modelled by a single diode model whose output current equations is given Equation (1), where  $I_{pv}$  is output current,  $I_p$  is light generated current and  $I_d$  is diode current. Light generated current is a function of solar irradiance (G) and temperature (T), while diode current is a function of temperature and diode voltage ( $V_d$ ). The parameters of the solar PV array and its associated DC-DC converter for time-domain simulations are given in Table 1.

$$I_{pv} = I_p(G, T) - I_d(T, V_d,)$$
 (1)

**Table 1** Time-domain simulation parameters

<b>PV Array Parameter details</b>	
Diode Ideality Factor	0.98
Voltage Temperature Coefficient	-0.36
Current Temperature Coefficient	0.10
Open Circuit Voltage	508.2
Short Circuit Current	666.4
Voltage at MPP	406
Current at MPP	624.75
Series connected modules per string	14
Parallel strings	85
Maximum Power (W)/module	213.15
<b>PV DC-DC Converter</b>	
Input Capacitor	50000 $\mu$ F
Output Capacitor	10 F
Inductor	25 mH

### 2.1.1 Neural network-based intelligent maximum power point tracking

In order to operate the solar photovoltaic system in the MPPT mode of operation, maximum power point algorithms are used [27]. Authors in [28] discussed partial shading effect on PV and used particle swarm optimization technique for maximum power point tracking. Algorithms like perturb and observe, incremental conductance method are mainly used for MPPT operation due to the ease of use. However, these algorithms are having an issue in that they generate oscillations around the maximum power point. These disadvantages are overcome by using artificial intelligence techniques like neural network-based maximum power point tracking. Neural networks have the capability of learning, due to which they have good tracking properties. Apart from tracking they are used for multiple applications like forecasting etc [29, 30]. The DC-DC converter interfacing PV array with the DC bus as shown in Figure 2 is provided controlled gate pulses via PWM control strategy that operated the PV at its maximum power point.

As shown in Figure 3, the feed-forward neural network is employed to operate the PV at its maximum power point with temperature and solar irradiance as its input parameters and the voltage corresponding to maximum power point as its output. Equations that are modelled numerically, experimentally and by some mathematical relations of PV modelling are used to generate the random data for neural network training. Different PV arrays have different characteristics, and it has been proved experimentally that the open-circuit voltage and short circuit current of PV array are related

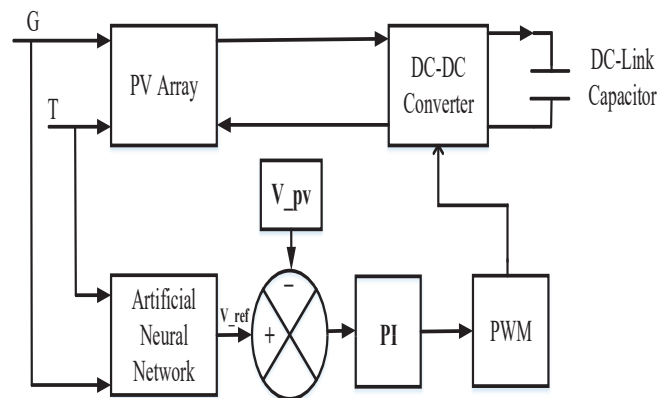


**Figure 2** Neural Network-Based MPPT Tracking control.

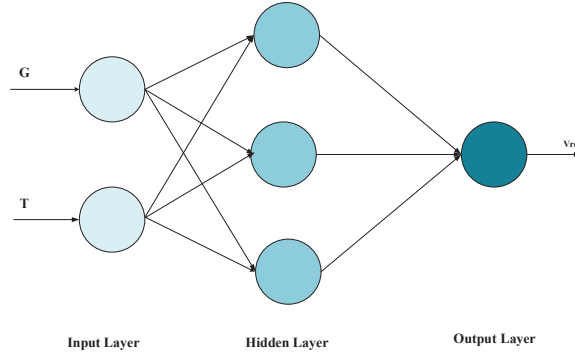


**Figure 3** Topology of feed forward neural network.

to MPP voltage and current by linear relations as given in Equation (2) and Equation (3), where  $C_1$  and  $C_2$  are voltage and current factors. These values depend on the characteristics of PV array; however, typical values for  $C_1$  are in the range of 0.71-0.78 and that of  $C_2$  are in the range of 0.78-0.92 [31]. Short circuit current and open-circuit voltage are related to the solar irradiance and temperature through the Equation (4) and Equation (5) respectively, where  $G_s, I_{sc,S}, V_{oc,S}, T_s$  are solar irradiance, short circuit current, open-circuit voltage and temperature at standard conditions.  $k, N_s, n, q, \alpha$  are Boltzmann's constant, number of solar cells in series in a module, diode ideality factor and charge of the electron and thermal voltage coefficient respectively [32]. The majority of the parameter details are provided in the data sheets of a particular manufacturer. The minimum temperature was considered to be at  $1^\circ C$  and maximum at  $40^\circ C$ , minimum and maximum irradiance was taken as  $50W/m^2$  and  $1000W/m^2$  respectively. These modelling equations are used to create the random data sets (1000 input/output data pairs) for the training of neural networks. The surface plot of the training input and target data is given in Figure 4. The output of a neural network is  $V_{ref}$  i.e. the voltage corresponding to the MPP.

$$V_{mp} = V_{ref} = C_1 V_{oc} \quad (2)$$

$$I_{mp} = C_2 I_{sc} \quad (3)$$

$$I_{sc} = \frac{G}{G_s} [I_{sc,S} + \alpha(T - T_s)] \quad (4)$$

$$V_{oc} = V_{oc,S} + \frac{N_s k T n}{q} \ln(G) + \alpha(T - T_s) \quad (5)$$

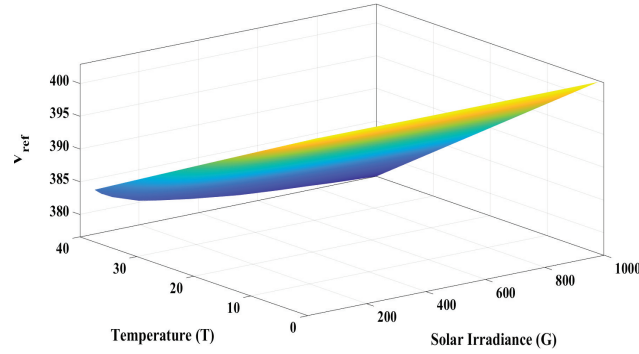


**Figure 4** Surface plot of Input and Output target data.

**Table 2** Effect of training algorithms and stacking in neural networks

Neural Network Topology	Training Algorithm	Data Samples	MSE	R	
3-Neurons in Hidden Layer	Levenberg-Marquardt	Training	700	1.3817e-3	9.9998e-1
		Validation	150	1.0577e-3	9.9998e-1
		Testing	150	8.6404e-4	9.9999e-1
3-Neurons in Hidden Layer	Scaled Conjugate Gradient	Training	700	1.4735e-2	9.9984e-1
		Validation	150	1.7901e-2	9.9982e-1
		Testing	150	1.5737e-2	9.9985e-1
5-Neurons in Hidden Layer (Stacked Neural Network)	Levenberg-Marquardt	Training	700	5.6266e-5	9.9999e-1
		Validation	150	5.8272e-5	9.9999e-1
		Testing	150	5.3177e-5	9.9999e-1

In [33], it was found that conventional perturb and observe MPPT technique is less accurate than neural network-based MPPT method. In neural network based MPPT tracking the mean square error in estimating maximum power point is reduced by 74.3% compared to conventional technique like perturb and observe. Extending the work to validate the effect of stacking and training algorithms on the accuracy of neural networks, a comparative study was made as given in Table 2. It was concluded that using the Levenberg-Marquardt training algorithm for 1-5-1 topology resulted in the least mean square error and high regressor value. For a given solar irradiance profile, as shown in Figure 13, the output  $V_{ref}$  is compared between 1-3-1 topology and 1-5-1 topology, and it is very clear from Figure 5. that 1-5-1 is tracking the MPPT voltage more accurately. Extended illustrative discussion on the use of conventional MPPT and neural network-based MPPT methods is essential for economic analysis. Although deep neural networks with more neurons in hidden layers or sometimes even more layers are more accurate, their hardware implementation is costly and complex. Therefore, it is essential to trade-off between the benefits of neural networks and conventional MPPT

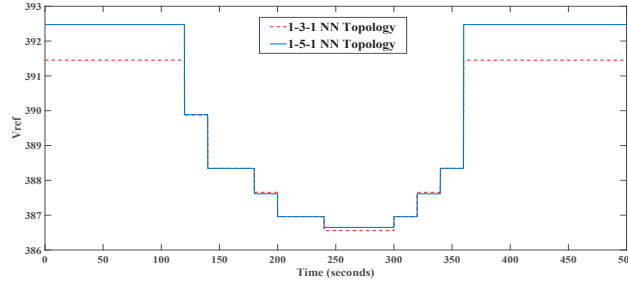


**Figure 5** Neural network output voltage.

methods. More work can be focused on this area in future. However, for the time being, based on the preliminary examination, it is recommended to use conventional perturb and observe method for integrated energy systems of smaller power rating. For PV-based integrated energy systems of large power rating, neural network-based MPPT techniques will be more advantageous.

## 2.2 Energy Storage

Energy storage is critical for non-dispatchable power sources like wind and solar, as it helps overcome the intermittency associated with renewable power sources. There are many energy storage technologies available like pumped hydropower, flywheels, compressed air, stored hydrogen, super-capacitors, superconducting magnetic energy storage (SMES), batteries etc. Among the available energy storage technologies, batteries are the most preferred for renewable-based microgrids. The Lithium-Ion battery has many advantages like high energy density, low self-discharge, fast response time (milliseconds) and lightweight, making it a natural choice for micro power systems.

Series parallel combination of the batteries helps in choosing the appropriate voltage, current and battery capacity levels. The Lithium-Ion battery is modelled as a current-controlled voltage source in series with internal resistance for time-domain simulations. Battery SOC is an important parameter that can not be measured directly; hence needs some estimation techniques like Kalman filtering, coulomb counting etc. Battery SOC estimation by coulomb counting is given by Equation (6). Time-domain simulation parameters of battery and associated bidirectional power converter is given in Table 3.

$$SOC = SOC_{ini} + \frac{1}{C_{nom}} \int i_b dt \quad (6)$$

**Table 3** Time-domain simulation parameters

<b>Lithium-Ion Battery Parameters</b>	
Nominal Voltage (V)	120
Rated Capacity (Ah)	420
Initial state-of-charge (%)	70
Battery Response Time (s)	0.009
<b>Battery DC-DC Converter</b>	
Inductor	25 mH

**Table 4** Grid converter parameters

Filter Capacitor	10 F
DC-DC Converter Output Capacitor	10 F
DC-DC Converter Inductor	25 mH

### 2.3 Distribution Network (Feeder line)

The output of the distribution transformer is usually a three-phase four-wire system, with each phase operating at a voltage of 220 V and 50 Hz frequency. Distribution network feeder line is available and is connected to DC bus via diode bridge rectifier and DC-DC buck converter for the proposed integrated energy system. The DC-DC buck converter supplies the power from the grid to the DC bus at a constant voltage level. Time-domain simulation parameters of converters are given in Table 4. The power is imported from the distribution network only during the night hours when the demand for the power is low. This imported power is utilised for hydrogen generation and provides ancillary services. An important assumption is made that the power flow in the distribution networks comes from some renewable power source like the wind.

### 2.4 PEM Electrolyzer and its Modelling

An electrolyser is a device that produces hydrogen from water through an electro-chemical process. High current density, low maintenance, noiseless operation, and compact size over alkaline electrolysers makes Proton exchange membrane (PEM) electrolysers a better choice. PEM electrolyser operates from DC power supply. However, to generate the hydrogen from the renewable energy-based hybrid system, the PEM electrolyser needs to be modelled to be connected with the DC bus. The equations that are used to model and develop the electrical equivalent circuit given in Figure 6 for PEM electrolyser are given below where  $R_{i0}$ ,  $T_0$ ,  $p_0$ ,  $e^{rev0}$  represent

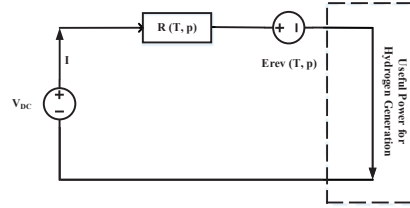


**Figure 6** Electrical equivalent circuit for PEM electrolyzer.

the reference resistance, reference temperature ( $20^{\circ}C$ ), reference pressure (1 atm) and reference reverse voltage respectively. Both non-linear resistance and reversible DC voltage are functions of temperature and pressure as given by equations Equation (7) and Equation (8), respectively [8]. Equation (9, 10) represents the linear relation for the current. PEM electrolyser is modelled as a controlled current sink through non-linear Equation (11). In Equation (7), the non-linear term represents the activation region, and it vanishes as the current builds up and the electrolyser starts to operate in the ohmic region (Linear region). Hydrogen production rate is generally a function of input current given by Equation (12). The voltage and current rating for a single PEM cell is 2 V and 1 A. The operating temperature and pressure for the electrolyser are considered to be  $25^{\circ}C$  and 1 atm, respectively. For time-domain simulations the parameters of the electrolyser are given in Table 5.

$$R(T, p) = R_{i0} + k \ln\left(\frac{p}{p_0}\right) + dR_t(T - T_0) \quad (7)$$

$$E_{rev}(T, p) = e^{rev0} + R(273 + T)\left(\frac{1}{2F}\right) \ln\left(\frac{p}{p_0}\right) \quad (8)$$

$$I(T, p) = 0 \quad \text{if } V_{DC} \leq E_{rev}(T, p) \quad (9)$$

$$I(T, p) = [V_{DC} - E_{rev}(T, p)]\left(\frac{1}{R(T, p)}\right) \quad \text{if } V_{DC} \geq e_{rev}(T, p) \quad (10)$$

$$I(T, p) = \frac{[V_{DC} - E_{rev}(T, p)](1 - e^{\frac{-5I}{0.02}})}{R(T, p)} \quad \text{if } V_{DC} \geq e_{rev}(T, p) \quad (11)$$

$$PH_2 = IV_{DC} \quad (12)$$

**Table 5** PEM electrolyzer configuration details

Power Rating	100 kW
Input Voltage	240 V
Input Current	416.666 A
No. of PEM Electrolyzer cells in series	140
No. of PEM Electrolyzer cells in parallel	570
Operating Pressure	1 atm
Operating Temperature	20°C

## 2.5 Hydrogen Storage

Generally, hydrogen is stored in two ways: either in gaseous form or in liquid form. A cryogenic system is needed when stored in liquid form and hence makes storage costly. High or medium pressure tanks store gaseous hydrogen under normal operating temperatures. New alternatives are emerging in the form of metal hydrides, underground hydrogen storage, etc., for bulk storage of hydrogen [18, 34].

## 3 Optimization for Integrated Energy Systems

In comparison to fossil fuel-based micro powers systems, renewable energy-based micro power systems are costlier. However, to encourage and scale up the use of renewable energy for green hydrogen generation, the cost of hydrogen generation needs to be reduced. This objective can be achieved by using the proper optimization method. As discussed earlier, the tool used to perform the optimization process for the proposed hybrid topology for green hydrogen generation is HOMER. In HOMER, the optimization algorithm used is “Grid search”, which helps in calculating the optimal sizing of the system components based on the user-defined control dispatch strategy. The dispatch strategy chosen for the current work is load-following. The optimization function in this work is to calculate Net Present Cost (NPC) and Cost of Hydrogen (COH) subject to system input parameters and select the best optimal system configuration based on least values of NPC and COH. Equation (13) and Equation (14) are used for calculating NPC and COH respectively [4, 35–37]. The net NPC of a particular system configuration is the sum of individual NPC of each system component. The NPC of each system component is defined as the sum of initial capital cost, replacement cost, operation and maintenance cost minus the salvage and revenues that it

earns over the lifetime of a project.

$$NPC = \frac{C_{annual}}{CRF_{i,R_p}} \tag{13}$$

$$COH = \frac{NPC}{H_t} \tag{14}$$

where  $C_{annual}$  is the annual total cost i.e annualised value of net NPC considering capital recovery factor, CRF is the capital recovery factor which is a function of  $i$  and  $R_p$ ;  $i$  is the annual interest rate set as 6% and  $R_p$  is the project lifetime which is set as 20 years in this work, and  $H_t$  is total hydrogen produced over lifetime.

### 3.1 Input Data for Optimization

The feasibility of PV-based microgrid for various applications depends on many factors like geographical location, sunshine hours, solar irradiance, load deviation etc. But these factors are stochastic and are not in the control of the system operator or designer. Those parameters on which the designer has control are known as decision variables. The decision variables in microgrids are generally system component sizes, quantities, and cost. A real case study was performed for the location with longitude and latitude as  $74.75^\circ E$ ,  $34.05^\circ N$  (Srinagar, J&K, India), respectively, to check the technical and economic feasibility of the proposed system configuration for hydrogen generation. Figure 7 shows the monthly average solar irradiance for the location considered [38]. Table 6 shows the input data for the optimization process. The different system component sizes, quantities, cost and dispatch

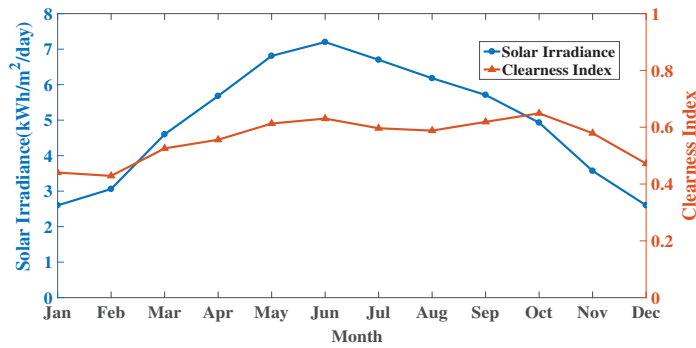


Figure 7 Monthly average solar irradiance.

**Table 6** System input data for optimization

<b>Solar Photovoltaic</b>			
Cost/kW	Capital (\$)	Replacement (\$)	O&M (\$)
	850	850	9
Sizes to consider	250 kW, 300kW, 400kW, 500 kW, 600 kW		
Lifetime	20 years		
Derating factor	85%		
Tracking system	Horizontal Axis, daily adjustment		
<b>Battery</b>			
Cost/battery	Capital (\$)	Replacement (\$)	O &M (\$/yr)
	150	150	5
Number of batteries to consider	20, 40		
Number of batteries per string	20		
Voltage rating/battery	12 V		
Nominal capacity	200 Ah		
Battery Type	Vision 6FM200D		
<b>Grid</b>			
Rate	Power Price (\$/kWh)	Sellback Rate (\$/kWh)	Demand Rate \$/kW/mo.
Peak-Hours	0.0504	0	0.694
Off-peakhours	0.0412	0	0.694
All ( $CO_2$ , CO, $SO_2$ , $NO_x$ , particulate matter (PM) emission factor	0 g/kWh		
Purchase Capacity	100 kW		
Sale Capacity	0 kW		
<b>Power Converter (Rectifier)</b>			
Cost/kW	Capital (\$)	Replacement (\$)	O & M(\$)
	350	350	0
Size	120 kW		
Efficiency	95%		
<b>DC Electrolyzer</b>			
Cost/kW	Capital (\$)	Replacement (\$)	O&M (\$/yr)
	560	500	12
Sizes to consider	100 kW		
Lifetime	10 yr		
Efficiency	65%		
<b>Hydrogen Tank</b>			
Cost/kg	Capital (\$)	Replacement (\$)	O&M (\$)
	83	70	2
Sizes to consider (kg)	500, 1000, 5000, 10000, 20000		

strategy, acts as a search space for the grid search algorithm. Solar irradiance profile and load data act as the system inputs for the optimisation process. An annual interest rate of 6% is considered from the economic point of view. There is no sell back power to the grid from a control point of view. The battery storage acts as a balance of the system that makes sure that the electrolyser is operated at its rated capacity of 100 kW. It generates 1.65 kg of hydrogen. HOMER performs the system optimisation, system simulation, and sensitivity analysis of the system. Simulations of the proposed integrated energy system are performed yearly, with a time step of one hour. Sensitivity analysis is performed to do the optimisation multiple times so that the impact of the parameter changes like grid energy cost, fuel cost etc., that are dynamic in nature can be considered [39].

**Table 7** Optimal design configurations

Optimal Designs	PV (kW)	Battery Vision 6FM55D Quantity	Grid (kW)	Electrolyzer (kW)	Hydrogen Tank (kg)	Total NPC (\$)	COH (\$/kg)
OD1	250	20	100	100	500	749904	4.806
OD2	250	40	100	100	500	757362	4.853
OD3	300	20	100	100	500	787814	5.048
OD4	300	40	100	100	500	795243	5.092
OD5	250	20	100	100	1000	800691	5.132
OD6	250	40	100	100	1000	808149	5.178
OD7	300	20	100	100	1000	838601	5.373
OD8	300	40	100	100	1000	846030	5.417
OD9	400	20	100	100	500	869878	5.569
OD10	400	40	100	100	500	877303	5.610
OD11	400	20	100	100	1000	920665	5.894
OD12	400	40	100	100	1000	928090	5.935
OD13	500	20	100	100	500	956917	6.122
OD14	500	40	100	100	500	964301	6.159
OD15	500	20	100	100	1000	1007704	6.447
OD16	500	40	100	100	1000	1015089	6.483
OD17	600	20	100	100	1000	1097292	7.017
OD18	600	40	100	100	1000	1104680	7.049
OD19	250	20	100	100	5000	1206989	7.736
OD20	250	40	100	100	5000	1214447	7.781
OD21	250	20	100	100	10000	1714862	10.9
OD22	259	40	100	100	10000	1722320	11.0

### 3.2 Optimization Results and Discussion

Based on the input data, the grid search algorithm was able to search through many candidates and find the optimal design configurations. Table 7 shows some of the essential optimal design configurations with the best optimal configuration at the top with special features of having the lowest net present cost and cost of hydrogen. Here in the proposed structure, it was assumed that there is a maximum hydrogen load demand of 1.65 kg per hour with random variation of  $\pm 10\%$ . Since hydrogen loads are future loads, it is challenging to predict the hydrogen load demand. However, hydrogen loads like fuel cell-based electric vehicles, fuel cell-based backup power systems, and hydrogen usage in chemical and other industries can be considered the current hydrogen loads existing in the present smart world. Based on the optimization results obtained, a conclusion can be drawn that the cost of hydrogen not only depends on the system component sizes and quantities but has some other factors like power management and control strategy. Developing intelligent power management and control algorithms can reduce the cost of hydrogen and decrease component size. For future research work, intelligence can be added to optimization algorithms for effective and precise optimal designs.

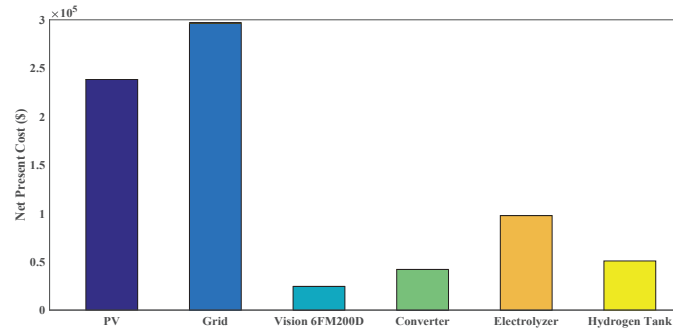


Figure 8 Cash flow summary.

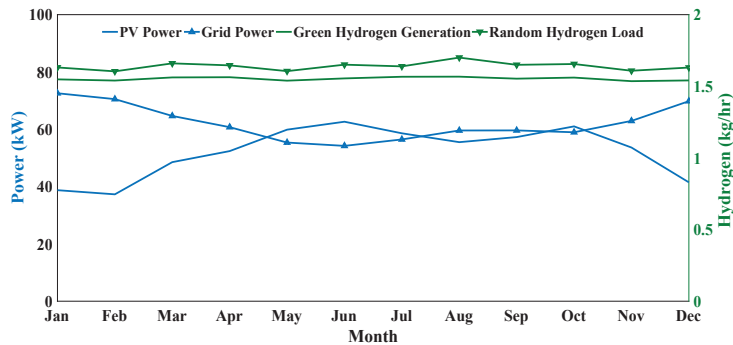


Figure 9 Power flow and hydrogen generation waveforms.

### 3.2.1 Simulation and Sensitivity Analysis

Apart from performing the optimisation, HOMER also performs the simulation and sensitivity analysis of the hybrid energy systems. The system simulation provides information about the cost, sizing and average power flow of each system component. Figure 8, shows the cash flow summary of the most optimal design configuration (OD1). The cash flow summary is the plot between the system components and NPC. From an electrical point of view, about 46% of electricity comes from solar PV, and the rest 54% comes from the local distribution grid as can be depicted from Figure 9. Battery plays an essential role in the overall balance of the system. The monthly average daily state of charge profile of the battery is shown in Figure 10. The minimum allowed charge level of the battery is 40%, and the maximum is 100%. The hydrogen load demand for the simulation purpose was 1.65kg/hr with random variability of  $\pm 10\%$ . As per the simulation

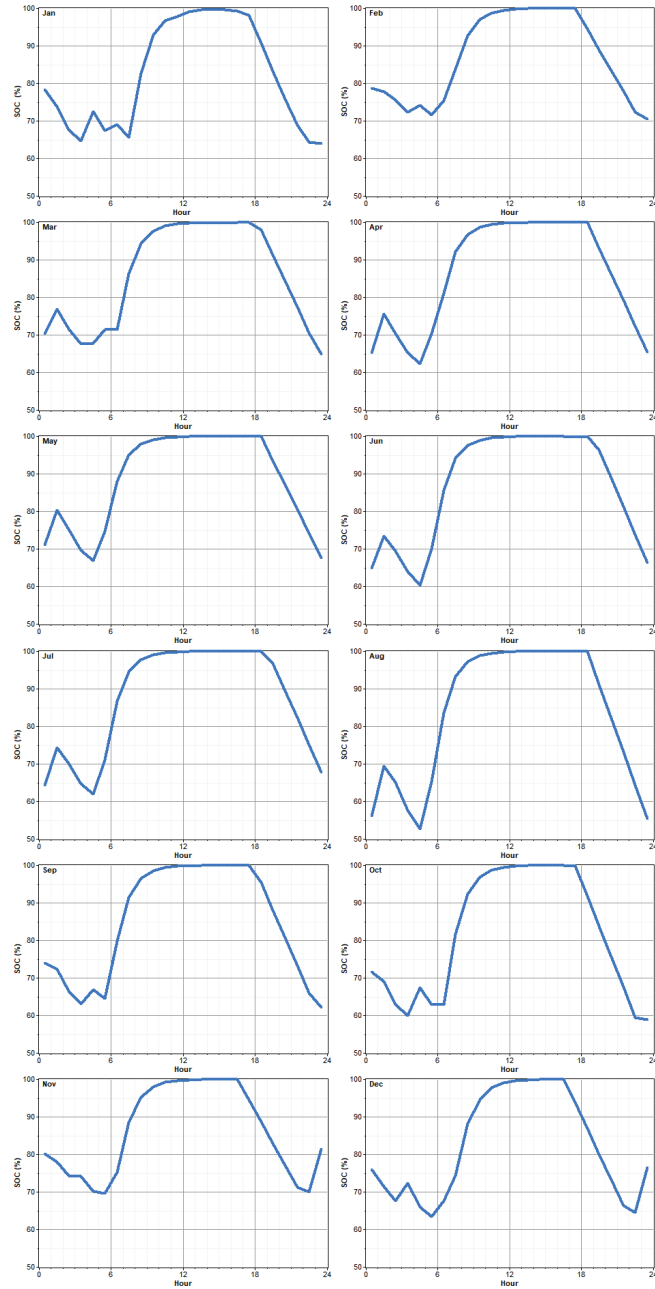


Figure 10 Battery state of charge daily profile.

results, hydrogen load demand was met with a shortage of 779 kg/yr (5.41%), with total hydrogen generation from a 100 kW electrolyser at 13,603 kg/yr. The unmet hydrogen is not because of power shortage but because of the limited capacity of the electrolyser. There is an excess of 14% electricity from the most optimal configuration. For future research and design purposes, it is recommended that the compressor utilise the extra power to store more hydrogen if the plant is scaled up. Sensitivity analysis is performed to check the effect of non-decision variables like load demand, solar irradiance, fuel price etc., that are not in the control of the designer. In this simulation, unmet hydrogen load with values of (30%, 40%, 60%, 80%) was considered the sensitivity variable; it was found that un-met load demand does not affect the cost of hydrogen. It can affect it only if the penalty factor is considered for the un-met load demand in the design process.

#### **4 Customized Power Management & Control Algorithm for Economical and Continuous Hydrogen Production**

The primary role of the power management and control algorithm is to generate reference power commands for the various power sources in integrated energy systems so that continuous power is supplied to the electrolyser for hydrogen production. Solar irradiance, wind speed, load changes, power prices fluctuations are some of the parameters that make renewable energy systems uncertain. Any change in these parameters leads to the power imbalance in the system that demands the design of efficient and effective power management and control algorithms. These algorithms control the system and help in switching on and off different power sources as per the generated reference power commands. Algorithm 1 represents the Customized Power Management and Control algorithm for economic and continuous hydrogen production.

### **5 Power Converters and Their Interfacing**

#### **5.1 AC-DC Rectifiers and DC-DC Converter**

Diode bridge rectifiers find applications in the design of power supplies, motor drives etc., as they have low cost compared to controlled rectifiers. In diode bridge rectifiers, the power flow is uni-directional, i.e. from the AC source to the DC side. A large capacitor is assumed to be on the DC side to

---

**Algorithm 1** Power Management and Control Algorithm for economic and continuous hydrogen production.

---

1: Power-balance equation for the proposed system configuration is given

$$P_{PV} \pm P_B + P_G = P_{EL} \quad (15)$$

2: If  $P_{PV} = 0$ , there are two alternatives to meet electrolyser power demand.

A1: Battery is initially assumed to be fully charged at 90% SOC. Let the battery supply power to electrolyser.

$$P_B = P_{EL} \quad (16)$$

A2: If  $P_{PV} = 0$  and battery has reached to its minimum allowed SOC level, import the power from the local distribution grid feeder.

Technical note: Battery bank should be sized in such a way that it has a back up of 4-5 hours, so that power can be imported from the distribution feeder network during off peak hours, it leads to economical operation and supports grid stability.

$$P_G = P_{EL} \quad (17)$$

3: If  $P_{PV} < P_{EL}$ , there are two alternatives to meet the electrolyser power demand.

A1: Let the electrolyser load demand be shared between solar photovoltaic power and battery power. This alternative is an option subject to battery SOC level.

$$\begin{aligned} \text{If } & B_{SOC} \geq B_{SOC_{min}} \\ & P_{PV} + P_B = P_{EL} \end{aligned} \quad (18)$$

A2: If battery SOC has reached to its lower end and PV power is very small, let the electrolyser power be shared between solar photovoltaic and grid power.

$$\begin{aligned} \text{If } & B_{SOC} \leq B_{SOC_{min}} , \\ & P_{PV} + P_G = P_{EL} \end{aligned} \quad (19)$$

$$P_{G,ref} = P_{EL} - P_{PV} \quad (20)$$

$$I_{G,ref} = \frac{P_{G,ref}}{V_{DClink}} \quad (21)$$

Technical Note: For time domain simulations  $B_{SOC_{min}}$  is considered to be at 65%. For practical integrated energy systems it is recommended to keep it at 20%.

4: If  $P_{PV} > P_{EL}$ . This is possible only when there is high solar irradiance or electrolyser is shut down for general maintenance. In this case, let the power imported from grid be zero and battery operate in charging mode.

$$P_G = 0 \quad (22)$$

$$P_{PV} - P_{EL} = P_B \quad (23)$$

5: If,  $P_{PV} > P_{EL}$  and  $Bat_{SOC} \geq SOC_{max}$ . Then in order to protect battery against over charging, it is better first to switch solar PV to off-MPPT mode, if still extra power exists dump load (Compressors for hydrogen production) should be activated.

$$V_{ref} = \frac{P_{EL}}{I_{PV}} \quad (24)$$


---

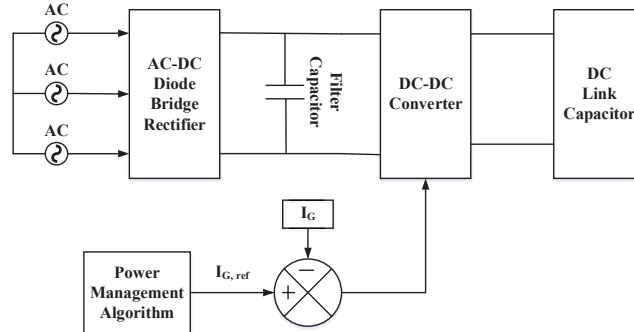


**Figure 11** Power electronic interface for grid power.

obtain the ripple-free DC output. Source inductance is used to avoid the distortion in the source current as diode bridge rectifiers draw distorted current from the utility side. Source inductance improves the power quality; however, it develops a commutation interval that reduces the average output voltage. As shown in Figure 11, in order to control the DC power of rectifiers, they are connected in series with DC-DC converters that are controlled through the closed-loop feedback control systems to get desired voltage and current levels so that power flow is controlled. To operate the DC-DC buck converter in a continuous conduction mode the values of L and C are designed by the Equations (25) and (27) respectively [40, 41] where,  $R_l$  is load resistance,  $d$  is duty ratio,  $F_s$  is switching frequency,  $\delta I$  and  $\delta V_o$  are ripple current and ripple voltage.  $\delta I$  is generally chosen between 10–20% of output current and  $\delta V_o$  as 5% of output voltage.

$$L = 10L_c \quad (25)$$

$$L_c = \frac{(1-d)R_l}{2F_s} \quad (26)$$

$$C = \frac{\delta I}{8F_s\delta V_o} \quad (27)$$

## 5.2 Bidirectional Buck-Boost DC-DC Converter

The Lithium-Ion battery is connected to the DC link via a bidirectional buck-boost converter as shown in Figure 12, so that there is power flow in both directions. Bidirectional buck-boost employs IGBT power electronic switches. The converter is controlled in such a way that constant DC link

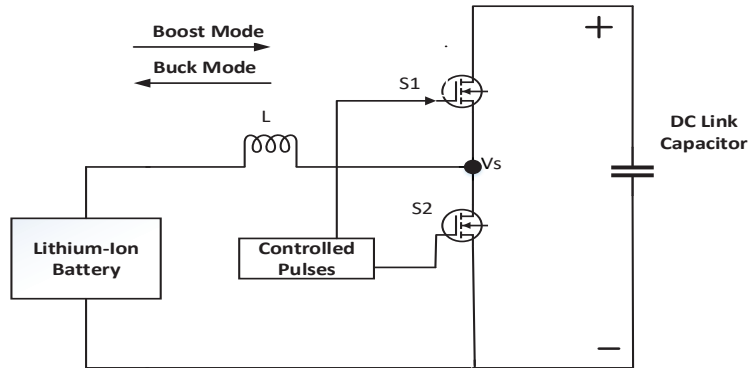


**Figure 12** Power electronic interface for lithium-ion battery.

voltage is maintained across the DC bus. Two switches of the converter are switched in such a way that if one is on with duty ratio  $D$ , another switch at the same time would be off with duty ratio as  $1-D$ . If  $V_s$  is greater than the battery terminal voltage, power flow will be from the DC link to the battery, and the bidirectional converter will operate in buck mode. Otherwise, if less, it will work in the boost mode. The size of the battery plays a vital role in the balance of the system as it helps in overcoming the intermittent nature of variable output power of renewable power sources and decides the system reliability.

## 6 Time-Domain Simulation Results and Discussions

In order to validate the effectiveness of the proposed power management and control algorithm for the proposed integrated energy system, time-domain simulations are carried out in MATLAB/Simulink environment. The time-domain simulations are run for a time period of 500s, considering different operating scenarios like availability of PV power, grid power and role of battery power in balancing the uncertainty associated with PV power. The component sizes and battery SOC band between minimum and maximum allowed SOC are scaled down for the time domain simulations so that simulations can be performed quickly to evaluate the response of power management algorithm. However for the practical cases the lower end of the battery SOC can be fixed around 10–20% and upper limit around 90%. The lower and upper limit of the battery SOC is subjected to battery management system that takes care of the battery state of health during the operation. The

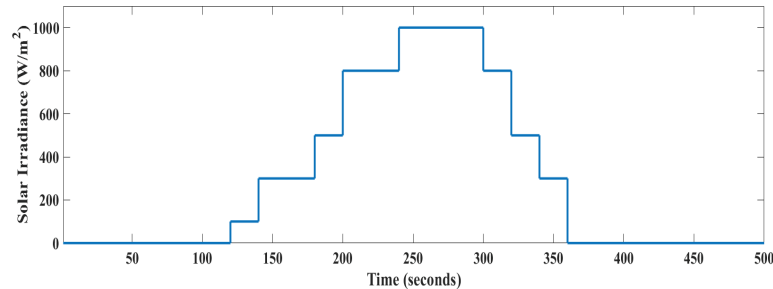


**Figure 13** Solar irradiance profile.

battery management system makes sure that battery deep discharging and battery overcharging are avoided to improve the battery lifetime. Random solar irradiance profile, as shown in Figure 13 is used for time-domain simulations so that the proposed system configuration can be deployed in any part of the world for developing distributed hydrogen production infrastructure. The solar irradiance profile considered for the time-domain simulations is hypothetical one used to check the effectiveness of power management and control algorithm for various modes of operation. In practical situation solar irradiance profile varies gradually. The power sources and storage devices are interfaced to DC link and electrolyser load via dc-dc converters. These DC-DC converters are modelled as switchings circuits for time-domain simulations purpose so that the control action and consensus-based decision making can be verified.

For the simulation purpose, PEM electrolyser is modelled as a controlled current sink through equations as mentioned in Section 2.4, across which a voltage level of  $240 \pm 10\%$  V given by Figure 14(a) is maintained during different operating scenarios and events. The local distribution grid is operated at a line voltage of 415 V and a frequency of 50 Hz. It is being assumed that the power in the local distribution grids is wind power as the future power networks will have more and more renewable power penetration only. Battery state of charge (SOC) waveform are represented by Figure 14(b). Figure 15(a) represents the electrolyser load demand. The PEM electrolyser is supplied power via three different power sources, viz solar PV, battery and grid power, depending on the operating condition, availability of power and the benefits associated with individual power sources. During initial conditions, it is being assumed that solar PV and grid power are zero and electrolyser is being supplied through the battery that has an initial state of charge level of 70%. As the battery continues to supply power to the electrolyser, it gets discharged;

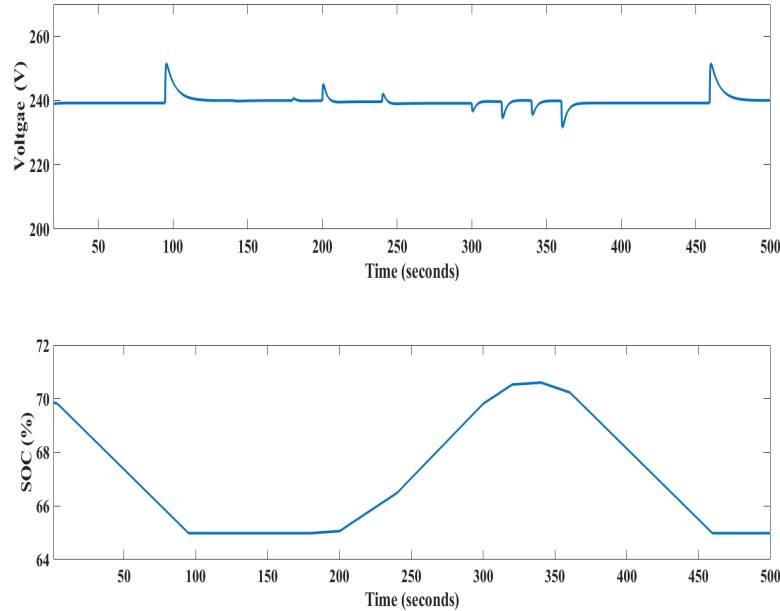


**Figure 14** (a) DC link voltage profile (b) battery state-of-charge waveform.

when it reaches the minimum allowed  $SOC_{min}$  ( $t = 95.2$  s), the grid power is turned on as shown in Figure 15(d). The local distribution grid continues to supply power of 100 kW to electrolyser till solar PV power ramps up. Here, the grid only supplies rated power to the electrolyser without feeding extra power to charge the battery that has reached its minimum allowed SOC limit. This  $SOC_{min}$  criterion is used to control the grid power. At time ( $t = 120$  s), solar irradiance increases to  $100W/m^2$  which increases solar power to 20 kW as given in Fig15 (b) thereby reducing grid power to 80 kW. At the time ( $t=140$  s), solar irradiance increases to  $300W/m^2$  which further increases the solar power to 64.7 kW and reduces grid power to a value of 35.3 kW; the battery power in this time interval is equal to 0. At the time ( $t = 180$  s), solar irradiance increases to  $500 W/m^2$  which increases the solar power to 108.3 kW and reduces grid power to zero. As now the solar power is slightly more than the rated power demand of electrolyser, the extra power is being diverted for battery charging. The grid continues to be in off mode, and at the time ( $t = 200$  s), solar irradiance increases to  $800 W/m^2$  which increases solar PV power to a value of 172 kW. Since PV power is more, the battery continues to operate in charging mode of operation with battery charging

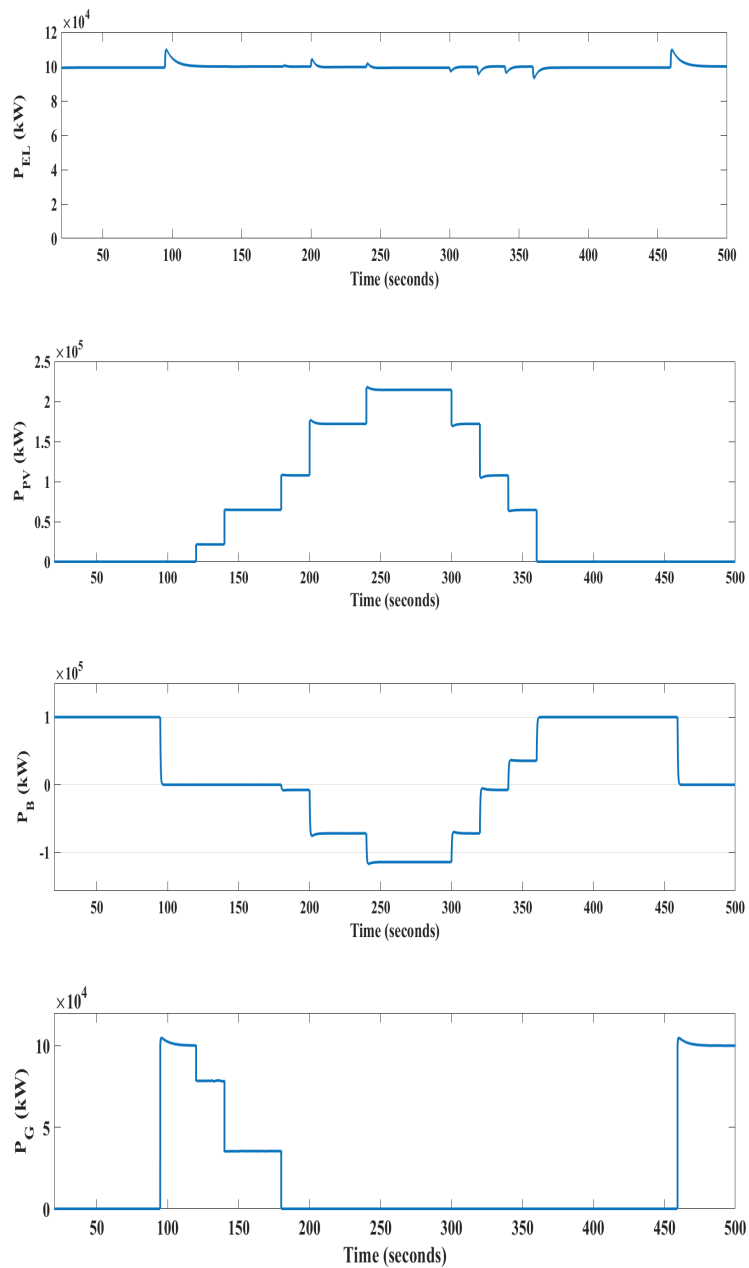


**Figure 15** (a) electrolyzer load demand (b) solar PV power (c) battery power (d) rectified grid power.

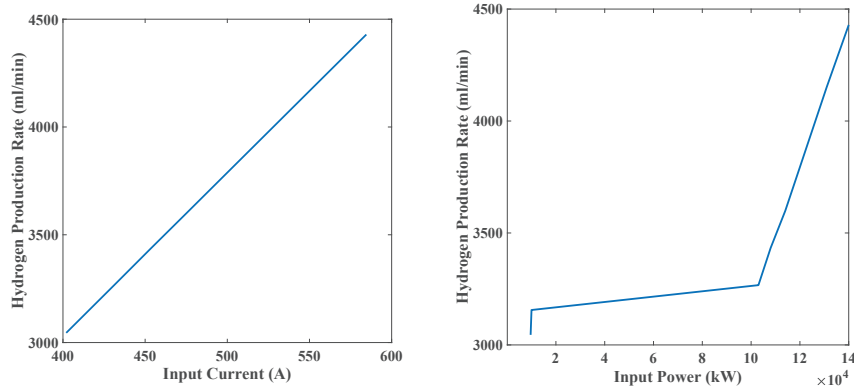


**Figure 16** (a) Input current vs hydrogen production rate (b) input power vs hydrogen production rate.

power equal to 72 kW. At the time ( $t = 240$  s), solar irradiance increases to the standard value of  $1000\text{W}/\text{m}^2$ , which increases solar PV power to a value of 214.5 kW. The battery charging power increases to a new value of 114.5 kW as shown in Figure 14(c). At the time ( $t = 300$  s), solar irradiance continues to decrease till  $t = 340$  s. In this time interval, Only solar PV continues to supply the electrolyser with the grid in off mode and battery in charging mode of operation. At the time ( $t = 340$  s), solar irradiance decreases to a new value of  $300\text{W}/\text{m}^2$ , which decrease the solar power to a value of 64.7 kW. Now the solar power is less than the load demand, and battery SOC is above the minimum allowed limits; now, the load power demand is shared between the battery and solar PV. At the time ( $t = 360$  s), solar PV power reduces to zero, and now the load power demand is supplied by the battery only as shown in Figure 15 (c). With solar PV power being zero and battery SOC reaching its lower allowed limit, at the time ( $t = 460$  s), the grid is turned on, and rated load power is imported from the grid. This cycle of turning on and off different power sources as per the power management algorithm commands continues to supply rated power to electrolysers and operates them round the clock for continued distributed green hydrogen production. This maintains the supply chain of green hydrogen and provides ancillary support to local distribution power networks that have renewable power penetration, especially during night hours when the power demand is less. Apart from ancillary services, it will help prevent negative power pricing where consumers are benefited from consuming power during excess power time zones. Corresponding to rated power of 100 kW the selected electrolyser

stack configuration produces hydrogen at a rate of 3156 ml/min. From the Figures 16(a) and 16(b) , it is clear that the relation between input current and hydrogen production rate is linear and relation between input power and hydrogen production rate is non-linear in nature for a particular electrolyser stack configuration.

## 7 Conclusion

The main intention behind this work was to study and analyse the renewable energy-based integrated energy systems for hydrogen production. Since uncertainty is associated with respective renewable power sources, link wind and solar PV. Developing an integrated energy system where individual power sources and energy storage devices work in coordination to overcome the stochastic nature becomes necessary. Power electronic circuitry was used to interface power and storage devices with the DC bus with the main aim of energy conversion and control. Developing distributed green hydrogen production infrastructure is a critical element for the transition towards a carbon-free society. In this paper, a new topology for an integrated energy system is proposed. The optimal sizing and costing of system components were performed to get the most optimal system configuration. Based on the optimisation results, it was concluded that the most optimal system configuration produced hydrogen at a rate of \$4.806/kg with a total NPC of \$ 749904. Apart from the optimisation, custom-based power management and control algorithm is proposed. Based on the proposed power management and control algorithm, time-domain simulations were carried out for a period of 500 s. The various parameters for decision making were battery SOC, availability of solar PV power, the tariff of grid power etc. The time-domain simulations confirmed the control and consensus-based decision making for operating the integrating energy system and providing stable and smooth power to the PEM electrolyser.

## 8 Future Work

- Deployment of electrolyzers across a distribution network and check its impact on the voltage and frequency during the high penetration of renewable power into distribution networks.
- Develop new optimization algorithms and compare results with the HOMER based optimizer.

- Perform dynamic modelling of PEM electrolyzers.
- Develop non-linear closed-loop control techniques for Converters.
- Perform experimental validation for the proposed microgrid configuration for green hydrogen production and develop research labs.

## Acknowledgment

The doctoral fellowship of corresponding author from Ministry of Human Resources Development (MHRD), New Delhi, India, via Grant No. 2017PHDFOESPRING46, is duly acknowledged.

## References

- [1] Dolf Gielen, Francisco Boshell, Deger Saygin, Morgan D. Bazilian, Nicholas Wagner, and Ricardo Gorini. The role of renewable energy in the global energy transformation. *Energy Strategy Reviews*, 24:38–50, 2019.
- [2] Filip Johnsson, Jan Kjärstad, and Johan Rootzén. The threat to climate change mitigation posed by the abundance of fossil fuels. *Climate Policy*, 19(2):258–274, 2019.
- [3] M. Farrokhhabadi, C. A. Cañizares, J. W. Simpson-Porco, E. Nasr, L. Fan, P. A. Mendoza-Araya, R. Tonkoski, U. Tamrakar, N. Hatziar-gyriou, D. Lagos, R. W. Wies, M. Paolone, M. Liserre, L. Meegahapola, M. Kabalan, A. H. Hajimiragha, D. Peralta, M. A. Elizondo, K. P. Schneider, F. K. Tuffner, and J. Reilly. Microgrid stability definitions, analysis, and examples. *IEEE Transactions on Power Systems*, 35(1):13–29, 2020.
- [4] Anastasios Oulis Rousis, Dimitrios Tzelepis, Ioannis Konstantelos, Campbell Booth, and Goran Strbac. Design of a hybrid ac/dc microgrid using homer pro: case study on an islanded residential application. *Inventions*, 3(3), 8 2018.
- [5] Sheikh Javed Iqbal Sheikh Suhail Mohammad. Improved dispatchability of solar photovoltaic system with battery energy storage. In *Proceedings of the 7th International Conference on Advances in Energy Research*, pages 1003–1013, 2020.
- [6] Barbara Widera. Renewable hydrogen implementations for combined energy storage, transportation and stationary applications. *Thermal Science and Engineering Progress*, 16:100460, 2020.

- [7] Sergio Matalucci. “<https://www.dw.com/en/a-57421078>”, how to be sure hydrogen is ‘green’ when it is comes in so many colors, accessed = 27 May 2021.
- [8] Ozcan Atlam and Mohan Kolhe. Equivalent electrical model for a proton exchange membrane (pem) electrolyser. *Energy Conversion and Management*, 52(8):2952 – 2957, 2011.
- [9] Marc Beisheim (accessed March 4, 2021). <https://www.globenewswire.com>, *Hydrogenics to Deliver World’s Largest Hydrogen Electrolysis Plant Air Liquide Selects Company for 20MW Installation*.
- [10] T. Nguyen, Z. Abdin, T. Holm, and W. Mérida. Grid-connected hydrogen production via large-scale water electrolysis. *Energy Conversion and Management*, 200:112108, 2019.
- [11] The Fuel Cells “<https://www.fch.europa.eu/soa-andtargets>” and Hydrogen Joint Undertaking. *Hydrogen production from renewable electricity for energy storage and grid balancing using PEM electrolyzers*, 2021 (accessed September 16, 2021).
- [12] A. Pena-Bello, E. Barbour, M.C. Gonzalez, M.K. Patel, and D. Parra. Optimized pv-coupled battery systems for combining applications: Impact of battery technology and geography. *Renewable and Sustainable Energy Reviews*, 112:978–990, 2019.
- [13] Venkatesh Boddapati and S. Arul Daniel. Design and feasibility analysis of hybrid energy-based electric vehicle charging station. *Distributed Generation and Alternative Energy Journal*, 37:41–72, 2022.
- [14] Ting Qiu and Jamal Faraji. Techno-economic optimization of a grid-connected hybrid energy system considering electric and thermal load prediction. *Energy Science & Engineering*, 9(9):1313–1336, 2021.
- [15] Haipeng Guan, Yan Ren, Qiuxia Zhao, and Hesam Parvaneh. Techno-economic Analysis of Renewable-based Stand-alone Hybrid Energy Systems Considering Load Growth and Photovoltaic Depreciation Rates. *Distributed Generation and Alternative Energy Journal*, 35:209–236, 2020.
- [16] Mehdi Jahangiri, Ahmad Haghani, Akbar Alidadi Shamsabadi, Ali Mostafaeipour, and Luis Martin Pomares. Feasibility study on the provision of electricity and hydrogen for domestic purposes in the south of iran using grid-connected renewable energy plants. *Energy Strategy Reviews*, 23:23–32, 2019.

- [17] Seyyed Ali Sadat, Jamal Faraji, Masoud Babaei, and Abbas Ketabi. Techno-economic comparative study of hybrid microgrids in eight climate zones of Iran. *Energy Science & Engineering*, 8(9):3004–3026, 2020.
- [18] Dimitris Ipsakis, Spyros Voutetakis, Panos Seferlis, Fotis Stergiopoulos, and Costas Elmasides. Power management strategies for a stand-alone power system using renewable energy sources and hydrogen storage. *International Journal of Hydrogen Energy*, 34(16):7081–7095, 2009. 4th Dubrovnik Conference.
- [19] A. Merabet, K. Tawfique Ahmed, H. Ibrahim, R. Beguenane, and A. M. Y. M. Ghias. Energy management and control system for laboratory scale microgrid based wind-pv-battery. *IEEE Transactions on Sustainable Energy*, 8(1):145–154, 2017.
- [20] Boualam Benlahbib, Nouredine Bouarroudj, Saad Mekhilef, Dahbi Abdeldjalil, Thameur Abdelkrim, Farid Bouchafaa, and Abelkader lakhdari. Experimental investigation of power management and control of a pv/wind/fuel cell/battery hybrid energy system microgrid. *International Journal of Hydrogen Energy*, 45(53):29110–29122, 2020.
- [21] Vaishalee Dash and Prabodh Bajpai. Power management control strategy for a stand-alone solar photovoltaic-fuel cell-battery hybrid system. *Sustainable Energy Technologies and Assessments*, 9:68–80, 2015.
- [22] Adel Choudar, Djamel Boukhetala, Said Barkat, and Jean-Michel Brucker. A local energy management of a hybrid pv-storage based distributed generation for microgrids. *Energy Conversion and Management*, 90:21–33, 2015.
- [23] Amin Hajizadeh, Samson G. Tesfahunegn, and Tore M. Undeland. Intelligent control of hybrid photo voltaic/fuel cell/energy storage power generation system. *Journal of Renewable and Sustainable Energy*, 3, 2011.
- [24] Naziha Harrabi, Mansour Souissi, Abdel Aitouche, and Mohamed Chaabane. Modeling and control of photovoltaic and fuel cell based alternative power systems. *International Journal of Hydrogen Energy*, 43(25):11442–11451, 2018. Alternative Energies for Sustainability.
- [25] T. Praveen Kumar, N. Subrahmanyam, and Maheswarapu Sydulu. Power management system of a particle swarm optimization controlled grid integrated hybrid pv/wind/fc/battery distributed generation system. *Distributed Generation and Alternative Energy Journal*, 36:141–168, 2021.

- [26] R. K. Sharma and S. Mishra. Dynamic power management and control of a pv pem fuel-cell-based standalone ac/dc microgrid using hybrid energy storage. *IEEE Transactions on Industry Applications*, 54(1):526–538, 2018.
- [27] Neetan Sharma, Farhad Ilahi Bakhsh, and Shivinder Mehta. Efficiency enhancement of a solar power plant using maximum power point tracking techniques. In *2018 International Conference on Computational and Characterization Techniques in Engineering Sciences (CCTES)*, pages 106–111, 2018.
- [28] Mehrun Nisa, Marya Andleeb, and Bakhsh Farhad Ilahi. Effect of partial shading on a pv array and its maximum power point tracking using particle swarm optimization. In *Journal of Physics: Conference Series*, volume 1817, page 012025. IOP Publishing, 2021.
- [29] Md. Tabrez, Md. Asif Hasan, Nidal Rafiuddin, and Farhad Ilahi Bakhsh. Upgrading cars running on indian roads: Analyzing its impact on environment using ann. In *2017 International Conference on Computing Methodologies and Communication (ICCMC)*, pages 1156–1160, 2017.
- [30] Bing Han, Mingxuan Li, Jingjing Song, Junjie Li, and Jamal Faraji. Optimal design of an on-grid microgrid considering long-term load demand forecasting: A case study. *Distributed Generation and Alternative Energy Journal*, 35:345–362, 2021.
- [31] Bo Zhao, Caisheng Wang, and Xuesong Zhang. *Grid-Integrated and Standalone Photovoltaic Distributed Generation Systems*, chapter 2, pages 17–41. John Wiley and Sons, Ltd, 2017.
- [32] Haider Ibrahim and Nader Anani. Variations of pv module parameters with irradiance and temperature. *Energy Procedia*, 134:276–285, 2017.
- [33] Samer Gowid and Ahmed Massoud. A robust experimental-based artificial neural network approach for photovoltaic maximum power point identification considering electrical, thermal and meteorological impact. *Alexandria Engineering Journal*, 59(5):3699–3707, 2020.
- [34] Michael Hirscher et. al. Materials for hydrogen-based energy storage – past, recent progress and future outlook. *Journal of Alloys and Compounds*, 827:153548, 2020.
- [35] Jamal Faraji, Hamed Hashemi-Dezaki, and Abbas Ketabi. Multi-year load growth-based optimal planning of grid-connected microgrid considering long-term load demand forecasting: A case study of tehran, iran. *Sustainable Energy Technologies and Assessments*, 42:100827, 2020.

- [36] S. Bennoua, A. Le Duigou, M.-M. Quéméré, and S. Dautremont. Role of hydrogen in resolving electricity grid issues. *International Journal of Hydrogen Energy*, 40(23):7231–7245, 2015.
- [37] Prachuab Peerapong and Bundit Limmeechokchai. Optimal electricity development by increasing solar resources in diesel-based micro grid of island society in thailand. *Energy Reports*, 3:1–13, 2017.
- [38] NASA Prediction Of Worldwide Energy Resources “<https://power.larc.nasa.gov/data-accessviewer/>”. *Multiple Data Access Options*, 2021 (accessed August 05, 2021).
- [39] Rohit Sen and Subhes C. Bhattacharyya. Off-grid electricity generation with renewable energy technologies in india: An application of homer. *Renewable Energy*, 62:388–398, 2014.
- [40] Ned Mohan, Tore M. Undeland, and William P. Robbins. *Power Electronics. Converters, Applications and Design*. John Wiley and Sons, Inc, third edition, 2003.
- [41] Robert W. Erickson and Dragan Maksimovic. *Fundamentals of Power Electronics*. Springer, 2ed edition, 2001.

## Biographies



**Sheikh Suhail Mohammad** received Bachelor’s degree in Electrical and Renewable Energy Engineering from the School of Engineering and Technology (SoET), Baba Ghulam Shah Badshah University Rajouri, Jammu and Kashmir, India in 2014. He received Master’s degree in Power Systems from Amity School of Engineering and Technology (ASET), Amity University Noida-New Delhi, India in 2016. He is currently pursuing Ph.D degree from the Department of Electrical Engineering, National Institute of Technology (NIT) Srinagar, India. His current research interests include optimization,

power management and intelligent control techniques for distributed generation and microgrids, application of artificial intelligence and machine learning techniques for integrated renewable energy systems.



**Sheikh Javed Iqbal** received Bachelor's degree in Electrical Engineering from Regional Engineering College (Now, National Institute of Technology) Srinagar, India in 1993. He received Master's degree in High Voltage Engineering from Indian Institute of Science (IISc.), Bangalore, India in 2002 and Ph.D degree from National Institute of Technology (NIT) Srinagar, India in 2014. He is presently working as Associate Professor at the Department of Electrical Engineering, NIT Srinagar, India. His current research interests include application of energy storage devices for power system dynamic applications, intelligent control techniques, wind and solar photovoltaic generation systems.